Metal−Organic Frameworks Based on Double-Bond-Coupled Di-Isophthalate Linkers with High Hydrogen and Methane Uptakes

Xi-Sen Wang,[†] Shengqian Ma,[†] Karsten Rauch,[‡] Jason M. Simmons,[§,||] Daqiang Yuan,[†] Xiaoping Wang,[⊥] Taner Yildirim,[§,||] William C. Cole,[†] Joseph J. López,[†] Armin de Meijere,[‡] and Hong-Cai Zhou*[,†]

Department of Chemistry and Biochemistry, Miami University, Oxford, Ohio 45056, Institut für Organische and Biomolekulare Chemie der Georg-August-Universität, Göttingen, Tammannstrasse 2, 37077 Göettingen, Germany, NIST Center for Neutron Research, Gaithersburg, Maryland 20899-6102, Department of Materials Science and Engineering, University of Pennsylvania, Philadelphia, Pennsylvania 19104, and Department of Chemistry, University of North Texas, Denton, Texas 76203

Received February 9, 2008. Revised Manuscript Received February 28, 2008. Accepted March 7, 2008

Solvothermal reactions of $Cu(NO_3)_2$ with azoxybenzene-3,3′,5,5′-tetracarboxylic acid (H_4aobtc) or *trans*-stilbene-3,3′,5,5′-tetracarboxylic acid (H_4sbtc) give rise to two isostructural microporous metal−organic frameworks, Cu_2(abtc)$(H_2O)_2$·3DMA (PCN-10, abtc = azobenzene-3,3′,5,5′-tetracarboxylate) and Cu_2(sbtc)-$(H_2O)_2$·3DMA (PCN-11, sbtc = *trans*-stilbene-3,3′,5,5′-tetracarboxylate), respectively. Both PCN-10 and PCN-11 possess significant enduring porosity with Langmuir surface areas of 1779 and 2442 m^2/g (corresponding to BET surface areas of 1407 or 1931 m^2/g, respectively) and contain nanoscopic cages and coordinatively unsaturated metal centers. At 77 K, 760 Torr, the excess gravimetric (volumetric) hydrogen uptake of PCN-10 is 2.34 wt % (18.0 g/L) and that of PCN-11 can reach 2.55 wt % (19.1 g/L). Gas-adsorption studies also suggest that MOFs containing C═C double bonds are more favorable than those with N═N double bond in retaining enduring porosity after thermal activation, although N═N has slightly higher H_2 affinity. The excess gravimetric (volumetric) adsorption at 77 K saturates around 20 atm and reaches values of 4.33% (33.2 g/L) and 5.05% (37.8 g/L) for PCN-10 and PCN-11, respectively. In addition to its appreciable hydrogen uptake, PCN-11 has an excess methane uptake of 171 cm^3(STP)/cm^3 at 298 K and 35 bar, approaching the DOE target of 180 v(STP)/v for methane storage at ambient temperature. Thus, PCN-11 represents one of the few materials that is applicable to both hydrogen and methane storage applications.

1. Introduction

Among various alternative fuels to gasoline and diesel, hydrogen and methane stand out. However, the lack of effective, economic, and safe on-board gas storage methods is one of the major technical barriers preventing hydrogen or methane from competing with conventional fuels.[1] For vehicular applications, the U.S. Department of Energy (DOE) has set storage targets for both methane and hydrogen. The target for methane storage is 180 cm^3 (STP) /cm^3 (35 bar, 298 K), which represents the energy density of adsorbed natural gas comparable to that of compressed natural gas used in current practice.[2] For hydrogen storage, the gravimetric (volumetric) system targets for near-ambient temperature (from −40 to 85 °C) and moderate pressure (less than 100 bar) are 6.0 wt % (45 g/L) for the year 2010 and 9.0 wt % (81 g/L) for 2015.[3] Several types of porous materials including single-walled carbon nanotubes, zeolites, and activated carbon have been extensively studied and tested as potential candidates for storage of methane[4] and hydrogen.[5] Although activated carbon materials possessing a methane storage capacity up to 200 cm^3(STP)/cm^3 have been

* To whom correspondence should be addressed. E-mail: zhouh@muohio.edu.
[†] Miami University.
[‡] Institut für Organische and Biomolekulare Chemie der Georg-August-Universität.
[§] NIST Center for Neutron Research.
[||] University of Pennsylvania.
[⊥] University of North Texas.

(1) (a) Hoogers, G. *Fuel Cell Technology Handbook*; 2003. (b) Schlapbach, L.; Züttel, A. *Nature* **2001**, *414*, 353. (c) Energy Policy Act of 1992 (EPAct).
(2) Burchell, T.; Rogers, M. *SAE Tech. Pap. Ser.* **2000**, 2001–2205.
(3) (a) DOE Office of Energy Efficiency and Renewable Energy Hydrogen, Fuel Cells & Infrastructure Technologies Program Multi-Year Research, Development and Demonstration Plan, available athttp://www.eere.energy.gov/hydrogenandfuelcells/mypp. (b) FY 2006 Annual Progress Report for the DOE Hydrogen Program, Nov 2006, available at http://www.hydrogen.energy.gov/annual_progress.html. (c) Satyapal, S.; et al. FY 2006 DOE Hydrogen Program Annual Merit Review and Peer Evaluation Meeting Proceedings, Plenary Session, available at http://www.hydrogen.energy.gov/annual_review06_plenary.html.
(4) (a) Muris, M.; Dupont-Pavlovsky, N.; Bienfait, M.; Zeppenfeld, P. *Surf. Sci.* **2001**, *492*, 67. (b) Dunn, J. A.; Rao, M.; Sircar, S.; Gorte, R. J.; Myers, A. L. *Langmuir* **1996**, *12*, 5896. (c) Quinn, D. F.; MacDonald, J. A. F. *Carbon* **1992**, *29*, 1097.
(5) (a) Smith, M. R.; Bittner, E. W.; Shi, W.; Johnson, J. K.; Bockrath, B. C. *J. Phys. Chem. B* **2003**, *107*, 3752. (b) Sudan, P.; Züttel, A.; Mauron, P.; Emmenegger, C.; Wenger, P.; Schlapbach, L. *Carbon* **2003**, *41*, 2377. (c) Nijkamp, M. G.; Raaymakers, J. E. M. J.; Van Dillen, A. J.; De Jong, K. P. *Appl. Phys. A: Mater. Sci. Proc.* **2001**, *72*, 619. (d) Schimmel, H. G.; Kearley, G. J.; Nijkamp, M. G.; Visser, C. T.; De Jong, K. P.; Mulder, F. M. *Eur. J. Chem.* **2003**, *9*, 4764. (e) Sandrok, G. *J. Alloys Compd.* **1999**, 293. (f) Cheetham, A. K.; Férey, G.; Loiseau, T *Angew. Chem., Int. Ed.* **1999**, *38*, 3268. (g) Davis, M. E. *Nature* **2002**, *417*, 813. (h) Fletcher, A. J.; Thomas, K. M. *Langmuir* **2000**, *16*, 6253. (i) Reid, C. R.; Thomas, K. M. *J. Phys. Chem. B* **2001**, *105*, 10619.

10.1021/cm800403d CCC: $40.75
Published on Web 04/15/2008

reported,[6] no material to date has met the U.S. DOE targets for both methane and hydrogen storage.

In the past decade, there is an escalation of interest in the study of metal−organic frameworks (MOFs) due to their fascinating structures and intriguing application potential.[7–15] Their exceptionally high surface areas,[8] uniform yet tunable pore sizes,[9] and well-defined adsorbate−MOF interaction sites[10,11b] make them suitable for methane and hydrogen storage. Various strategies to increase the adsorption capacity of MOFs, such as using pore sizes comparable to the adsorbed molecules, increasing surface area and pore volume,[6,11–13] utilizing catenation,[14] and introducing coordinatively unsaturated metal centers,[15] have been explored. Recently, inelastic neutron scattering and neutron powder diffraction as well as computational studies suggest that the choice of both metal centers and ligands can play an important role in tailoring the gas−framework interactions.[10,16] While ligands containing phenyl rings have been proved favorable for hydrogen and methane adsorption, those containing double-bond functionalities have rarely been studied in gas adsorption MOFs.[7h,i]

In this contribution, we present hydrogen and methane storage studies in MOFs containing nanoscopic cages based on two predesigned double-bond-coupled bis(isophthalate) ligands: azobenzene-3,3′,5,5′-tetracarboxylate (abtc) and *trans*-stilbene-3,3′,5,5′-tetracarboxylate (sbtc). Solvothermal reactions of $Cu(NO_3)_2$ with azoxybenzene-3,3′,5,5′-tetracarboxylic acid (H_4aobtc) or H_4sbtc give rise to isostructural PCN-10 and PCN-11 (PCN refers to porous coordination network), respectively. PCN-11 shows a remarkable excess volumetric (gravimetric) hydrogen uptake of 37.8 g/L (5.05 wt %) at 77 K and 20 bar and an excess methane uptake of 171 cm^3(STP)/cm^3 at 298 K and 35 bar, approaching the DOE target of 180 v(STP)/v for methane storage at ambient temperature.

2. Experimental Section

2.1. General Information. Commercially available reagents were used as received without further purification. Infrared spectra were obtained on a Perkin-Elmer Spectrum One FT-IR with a universal diamond ATR sampling accessory in the 650–4000 cm^{-1} region. Elemental analyses (C, H, and N) were performed by Canadian Microanalytical Service, Ltd. Thermogravimetric analysis (TGA) was performed under N_2 on a Perkin-Elmer TGA 7, and a Beckman Coulter SA3100 surface area analyzer was used to measure gas adsorption. NMR data were collected on a Bruker 200 or 300 MHz spectrometer. Powder X-ray diffraction patterns (PXRD) were obtained on a Rigaku Ultima III powder diffractometer in a parallel beam geometry using Cu Kα radiation with a routine power of 1600 W (40 kV, 40 mA).

2.2. H_4aobtc: Azoxybenzene-3,3′,5, 5′-tetracarboxylic Acid.[17] A mixture of 5-nitroisophthalic acid (2.10 g, 10 mmol), Zn (1.30 g, 20 mmol), and NaOH (0.80 g, 20 mmol) in a mixed solvent of ethanol (50 mL) and water (20 mL) was refluxed for 12 h. A yellow precipitate was obtained and collected by filtration. The solid was dissolved in 50 mL of NaOH (aq, 1 M), and the solution was filtered to remove an insoluble residue. The filtrate was acidified to pH = 3 with 3 M HCl (aq) to afford 1.59 g of H_4aobtc as a yellow solid (yield, 85%).

(6) (a) Wegrzyn, J.; Gurevich, M. *Appl. Energy.* **1996**, *55*, 71. (b) NSF press release (#07-011) http://www.nsf.gov/news/news_summ.jsp?cntn_id=108390. (c) Ma, S.; Sun, D.; Simmons, J. M.; Collier, C. D.; Yuan, D.; Zhou, H.-C. *J. Am. Chem. Soc.* **2008**, *130*, 1012.

(7) (a) Matsuda, R.; Kitaura, R.; Kitagawa, S.; Kubota, Y.; Belosludov, R. V.; Kobayashi, T. C.; Sakamoto, H.; Chiba, T.; Takata, M.; Kawazoe, Y.; Mita, Y. *Nature* **2005**, *436*, 238. (b) Dinca, M.; Long, J. R. *J. Am. Chem. Soc.* **2005**, *127*, 9376. (c) Pan, L.; Adams, K. M.; Hernandez, H. E.; Wang, X.; Zheng, C.; Hattori, Y.; Kaneko, K. *J. Am. Chem. Soc.* **2003**, *125*, 3062. (d) Dybtsev, D. N.; Chun, H.; Yoon, S. H.; Kim, D.; Kim, K. *J. Am. Chem. Soc.* **2004**, *126*, 32. (e) Pan, L.; Parker, B.; Huang, X.; Olson, D. H.; Lee, J. Y.; Li, J. *J. Am. Chem. Soc.* **2006**, *128*, 4180. (f) Llewellyn, P. L.; Bourrelly, S.; Serre, C.; Filinchuk, Y.; Férey, G, *Angew. Chem., Int. Ed.* **2006**, *45*, 7751. (g) Humphrey, S. M.; Chang, J.-S.; Jhung, S. H.; Yoon, J. W.; Wood, P. T. *Angew. Chem., Int. Ed.* **2006**, *46*, 272. (h) Liu, Y.; Eubank, J. F.; Cairns, A. J.; Eckert, J.; Kravtsov, V. Ch.; Luebke, R.; Eddaoudi, M. *Angew. Chem., Int. Ed.* **2007**, *46*, 3278. (i) Belof, J. L.; Stern, A. C.; Eddaoudi, M.; Space, B. *J. Am. Chem. Soc.* **2007**, *129*, 15202.

(8) (a) Chae, H. K.; Siberio-Pérez, D. Y.; Kim, J.; Go, Y. B.; Eddaoudi, M.; Matzger, A. J.; O'Keeffe, M.; Yaghi, O. M. *Nature* **2004**, *427*, 523. (b) Férey, G.; Mellot-Draznieks, C.; Serre, C.; Millange, F.; Dutour, J.; Surblé, S.; Margiolaki, I. *Science* **2005**, *309*, 2040.

(9) (a) Chen, B.; Ma, S.; Zapata, F.; Lobkovsky, E. B.; Yang, J. *Inorg. Chem.* **2006**, *45*, 5178. (b) Chen, B.; Ma, S.; Zapata, F.; Fronczek, F. R.; Lobkovsky, E. B.; Zhou, H.-C. *Inorg. Chem.* **2007**, *46*, 1233. (c) Ma, S.; Wang, X.-S.; Collier, C. D.; Manis, E. S.; Zhou, H.-C. *Inorg. Chem.* **2007**, *46*, 8499. (d) Ma, S.; Wang, X.-S.; Manis, E. S.; Collier, C. D.; Zhou, H.-C. *Inorg. Chem.* **2007**, *46*, 3432. (e) Ma, S.; Sun, D.; Wang, X.-S.; Zhou, H.-C. *Angew. Chem., Int. Ed.* **2007**, *46*, 2458.

(10) (a) Yildirim, T.; Hartman, M. R. *Phys. Rev. Lett.* **2005**, *95*, 215504. (b) Hartman, M. R.; Peterson, V. K.; Liu, Y.; Kaye, S. S.; Long, J. R. *Chem. Mater.* **2006**, *18*, 3221. (c) Peterson, V. K.; Liu, Y.; Brown, C. M.; Kepert, C. J. *J. Am. Chem. Soc.* **2007**, *128*, 15578. (d) Wu, H.; Zhou, W.; Yildirim, T. *J. Am. Chem. Soc.* **2007**, *129*, 5314.

(11) (a) Rowsell, J. L. C.; Yaghi, O. M. *Angew. Chem., Int. Ed.* **2005**, *44*, 4670. (b) Collins, D. J.; Zhou, H.-C. *J. Mater. Chem.* **2007**, *17*, 3154. (c) Sun, D.; Ma, S.; Ke, Y.; Collins, D. J.; Zhou, H.-C. *J. Am. Chem. Soc.* **2006**, *128*, 3896. (d) Ma, S.; Sun, D.; Ambrogio, M. W.; Fillinger, J. A.; Parkin, S.; Zhou, H.-C. *J. Am. Chem. Soc.* **2007**, *129*, 1858.

(12) (a) Noro, S.-i.; Kitagawa, S.; Kondo, M.; Seki, K. *Angew. Chem., Int. Ed.* **2000**, 1433. (b) Kondo, M.; Shimamura, M.; Noro, S.-i.; Minakoshi, S.; Asami, A.; Seki, K.; Kitagawa, S. *Chem. Mater.* **2000**, *12*, 1288. (c) Bourrelly, S.; Llewellyn, P. L.; Serre, C.; Millange, F.; Loiseau, T.; Ferey, G. *J. Am. Chem. Soc.* **2005**, *127*, 13519. (d) Eddaoudi, Kim, J.; Rosi, N.; Vodak, D.; Wachter, J.; O'Keeffe, M.; Yaghi, O. M. *Science* **2002**, *295*, 469.

(13) Dueren, T.; Sarkisov, L.; Yaghi, O. M.; Snurr, R. Q. *Langmuir* **2004**, *20*, 2683.

(14) (a) Pan, L.; Sander, M. B.; Huang, X.; Li, J.; Smith, M. R., Jr.; Bittner, E. W.; Bockrath, B. C.; Johnson, J. K. *J. Am. Chem. Soc.* **2004**, *126*, 1308. (b) Kesanli, B.; Cui, Y.; Smith Milton, R.; Bittner Edward, W.; Bockrath Bradley, C.; Lin, W. *Angew. Chem., Int. Ed.* **2005**, *44*, 72.

(15) (a) Chen, B. L.; Ockwig, N. W.; Millward, A. R.; Contreras, D. S.; Yaghi, O. M. *Angew. Chem., Int. Ed.* **2005**, *44*, 4745. (b) Lin, X.; Jia, J.; Zhao, X.; Thomas, K. M.; Blake, A. J.; Walker, G. S.; Champness, N. R.; Hubberstey, P.; Schroder, M. *Angew. Chem., Int. Ed.* **2006**, *45*, 7358. (c) Ma, S.; Zhou, H.-C. *J. Am. Chem. Soc.* **2006**, *128*, 11734. (d) Dincă, M.; Dailly, A.; Liu, Y.; Brown, C. M.; Neumann, D. A.; Long, J. R. *J. Am. Chem. Soc.* **2006**, *128*, 16876. (e) Dincă, M.; Han, W. S.; Liu, Y.; Dailly, A.; Brown, C. M.; Long, J. R. *Angew. Chem., Int. Ed.* **2007**, *46*, 1419. (f) Forster, P. M.; Eckert, J.; Heiken, B. D.; Parise, J. B.; Yoon, J. W.; Jhung, S. H.; Chang, J.-S.; Cheetham, A. K. *J. Am. Chem. Soc.* **2006**, *128*, 16846. (g) Mulfort, K. L.; Hupp, J. T. *J. Am. Chem. Soc.* **2007**, *129*, 9604. (h) Rowsell, J. L. C.; Yaghi, O. M. *J. Am. Chem. Soc.* **2006**, *128*, 1304. (i) Kaye, S. S.; Dailly, A.; Yaghi, O. M.; Long, J. R. *J. Am. Chem. Soc.* **2007**, *129*, 14176. (j) Frost, H.; Düren, T.; Snurr, R. Q. *J. Phys. Chem. B* **2006**, *110*, 9565.

(16) (a) Rowsell, J. L. C.; Eckert, J.; Yaghi, O. M. *J. Am. Chem. Soc.* **2005**, *127*, 14904. (b) Hubner, O.; Gloss, A.; Fichtner, M.; Klopper, W. *J. Phys. Chem. A* **2004**, *108*, 3019. (c) Liu, Y.; Brown, C. M.; Neumann, D. A.; Peterson, V. K.; Kepert, C. J. *J. Alloys Compd.* **2007**, *446–447*, 385.

(17) (a) Wang, S.; Wang, X.; Li, L.; Advincula, R. C. *J. Org. Chem.* **2004**, *69*, 9073. (b) Ebel, K.; Krueger, H.; Musso, H. *Chem. Ber.* **1988**, *121*, 323.

Scheme 1. Synthetic Route to H_4sbtc

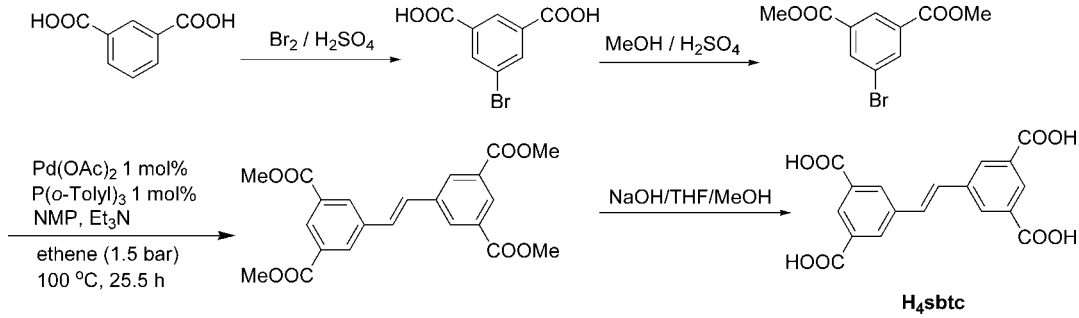

Scheme 2. Synthetic Route to H_4aobtc

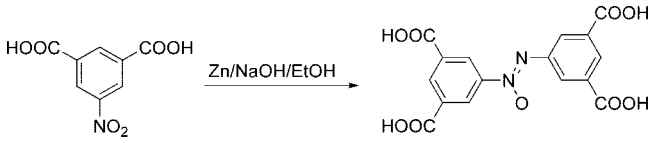

A solution of 10 mg of H_4aobtc in 1.5 mL of dimethylacetamide (DMA) was sealed in a Pyrex tube under vacuum and heated at 1 °C/min to 80 °C, kept at the temperature for 2 days, and cooled to room temperature at 0.1 °C/min. Colorless crystals of H_4aobtc suitable for single-crystal X-ray analysis were obtained. ^{1}H NMR (DMSO-d_6): 8.48 (t, ^4J = 1 Hz, 1 H), 8.65 (t, ^4J = 1 Hz, 1 H), 8.76 (d, ^4J = 1 Hz, 2 H), 8.90 (d, ^4J = 1 Hz, 2 H), 13.60 (s, br, 4 H).

2.3. Tetramethyl *trans*-Stilbene-3,3′,5,5′-tetracarboxylate.[18] A 300 mL glass autoclave was charged with dimethyl 3-bromoisophthalate (2.00 g, 7.32 mmol), palladium acetate (16.4 mg, 0.0732 mmol), and tris-*o*-tolylphosphine (44.5 mg, 0.146 mmol). The autoclave was closed, evacuated, and filled with nitrogen. The evacuation and filling with nitrogen was repeated four more times, and then anhydrous triethylamine (2.2 mL, 15.8 mmol) and anhydrous *N*-methylpyrrolidone (2.2 mL) were added under nitrogen. The autoclave was evacuated and filled with 1.5 bar of ethene, the pressure was released and then built up again, and this release and repressurization was repeated three more times in order to saturate the solvent with ethene. The contents of the autoclave were then kept under a pressure of 1.5 bar of ethene and stirred at 100 °C for 25.5 h. After having been cooled to ambient temperature, the autoclave valve was opened to release excess ethene, and the content was taken up in methylene chloride (100 mL). The solution was washed with water (3 × 50 mL), dried ($MgSO_4$), and concentrated under reduced pressure. The residue was subjected to column chromatography on silica gel (34 g) to yield 1.181 g (78%) of the title compound as a light yellow solid (R_f = 0.16, CH_2Cl_2), mp 215 °C. IR (KBr, cm^{-1}): 2956, 1735, 1727, 1435, 1347, 1328, 1245, 1210, 1127, 1014, 1000, 753. ^{1}H NMR (250 MHz, $CDCl_3$): δ = 3.98 (s, 12 H), 7.31 (s, 2 H), 8.38 (d, ^4J = 1.5 Hz, 4 H), 8.59 (t, ^4J = 1.5 Hz, 2 H). ^{13}C NMR (62.9 MHz, $CDCl_3$, add. DEPT): δ = 52.49 (+), 128.88 (+), 129.91 (+), 131.13 (C_{quat}), 131.61 (+), 137.37 (C_{quat}), 165.99 (C_{quat}). MS (EI, 70 eV) *m*/*z* (%) = 412 (M^+, 100), 381 (32), 175 (15). UV (CH_3CN): λ_{max} (lg ϵ) = 200.5 (4.5095), 234.5 (4.3540), 296.5 nm. Anal. Calcd for $C_{22}H_{20}O_8$ (412.4): C, 64.07; H, 4.89. Found: C, 64.13; H, 4.76.

2.4. H_4sbtc: *trans*-Stilbene-3,3′,5,5′-tetracarboxylic Acid. Tetramethyl *trans*-stilbene-3,3′,5,5′-tetracarboxylate (3.00 g) was suspended in 100 mL of THF/MeOH (v:v = 1: 1), and 20 mL of 10% NaOH solution was added. The mixture was stirred overnight. The pH value was adjusted to approximately 2 using hydrochloric acid. The resulting white precipitate was collected by filtration, washed with water, and dried under vacuum to give H_4sbtc (2.46 g, 95%). A solution of 10 mg of H_4sbtc in 1.5 mL of DMA was sealed in a Pyrex tube under vacuum, heated at 1 °C/min to 80 °C, kept at the temperature for 2 days, and cooled to room temperature at 0.1 °C/min. Colorless crystals suitable for single-crystal X-ray analysis were obtained. ^{1}H NMR (DMSO-d_6): 7.13 (s, 2 H), 8.39 (d, ^4J = 1.54 Hz, 2 H), 8.60 (t, ^4J = 1.54 Hz, 4 H).

2.5. Cu_2(abtc)(H_2O)$_2$·3DMA (PCN-10). A mixture of H_4aobtc (0.010 g, 2.67 × 10^{-5} mol) and $Cu(NO_3)_2$·2.5H_2O (0.025 g, 1.07 × 10^{-4} mol) in 1.5 mL of DMA was sealed in a Pyrex tube under vacuum and heated at 1 °C/min to 80 °C, kept at the temperature for 2 days, and cooled to room temperature at 0.1 °C/min. The resulting blue block crystals were washed with DMA several times to give PCN-10 with a formula of $Cu_2(C_{16}H_6N_2O_8)(H_2O)_2$·3$C_4H_9NO$ (0.011 g, yield 62%). IR (cm^{-1}): 2942 (w), 1601 (s), 1505 (w), 1445 (m), 1398 (m), 1372 (s), 1262 (m), 1188 (m), 1104 (w), 1060 (w), 1014 (m), 963 (w), 924 (w), 847 (w), 796 (w), 776 (s), 748 (w), 726 (s). Anal. Calcd for PCN-10: C, 43.19; H, 4.79; N, 8.99. Found: C, 43.37; H, 4.91; N, 8.72.

2.6. Cu_2(sbtc)(H_2O)$_2$·3DMA (PCN-11). The synthetic procedure is very similar to that of PCN-10 except that H_4sbtc (0.010 g, 2.67 × 10^{-5} mol) was used in place of H_4aobtc. PCN-11 has a formula of $Cu_2(C_{16}H_6N_2O_8)(H_2O)_2$·3$C_4H_9NO$ (0.012 g, yield 67%). IR (cm^{-1}): 3413 (w), 2934 (w), 1618 (s), 1502 (w), 1447 (w), 1396 (s), 1376 (s), 1287 (w), 1262 (m), 1188 (m), 1104 (w), 1057 (w), 1014 (m), 963 (w), 924 (w), 847 (w), 796 (w), 774 (s), 728 (s), 688 (w). Anal. Calcd for PCN-10: C, 43.19; H, 4.79; N, 8.99. Found: C, 43.37; H, 4.91; N 8.72.

2.7. X-ray Crystallography. Single-crystal X-ray structure determinations of H_4aobtc, H_4sbtc, and as-isolated PCN-10 and PCN-11 were performed at 213(2) K on a Bruker SMART APEX II diffractometer using graphite-monochromated Mo Kα radiation (λ = 0.71073 Å). Raw data for all structures were processed using SAINT, and absorption

(18) An incorrect variant of this procedure has previously been published without our consent, see: Rau, H.; Waldner, I. *Phys. Chem. Chem. Phys.* **2004**, *4*, 1776.

Table 1. Crystal Data[a] and Structure Refinement of H_4aobtc·4DMA, H_4sbtc·4DMA, and As-Isolated PCN-10 and PCN-11

	H_4aobtc·4DMA	H_4sbtc·4DMA	PCN-10	PCN-11
formula	$C_{32}H_{46}N_6O_{13}$	$C_{34}H_{48}N_4O_{12}$	$C_{16}H_{10}Cu_2N_2O_{10}$	$C_{18}H_{12}Cu_2O_{10}$
fw	722.75	704.76	517.34	515.36
cryst syst	triclinic	triclinic	rhombohedral	rhombohedral
space group	*P*-1	*P*-1	*R*-3	*R*-3
a, Å	6.289(3)	7.320(7)	18.799(15)	18.795(3)
b, Å	8.009(3)	10.709(10)	18.799(15)	18.795(3)
c, Å	18.625(7)	12.668(10)	30.61(4)	31.280(9)
α, deg	78.018(8)	65.560(18)	90.00	90.00
β, deg	88.648(9)	89.18(2)	90.00	90.00
γ, deg	89.537(8)	88.097(19)	120.00	120.00
V, Å^3	917.4(6)	903.6(14)	9374(16)	9569(3)
Z	1	1	9	9
ρ_{calcd}, g cm^{-3}	1.308	1.295	0.825	0.805
μ, mm^{-1}	0.102	0.098	1.048	1.025
GOF	1.459	1.248	1.01	0.93
R_1,wR_2 [b]	0.0926, 0.2956	0.1180, 0.3105	0.0557, 0.1537	0.0994, 0.2408

[a] Obtained with graphite-monochromated Mo Kα (λ = 0.71073 Å) radiation. [b] $R_1 = \Sigma\Delta F_o| - |F_o\Delta/\Sigma|F_o|$, and $wR_2 = \{\Sigma w(F_o^2 - F_c^2)^2]/[\Sigma w(F_o^2)^2]\}^{1/2}$.

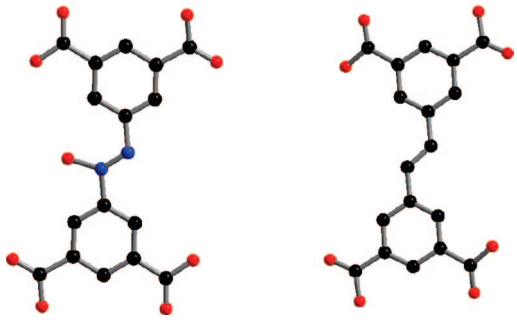

Figure 1. Crystal structures of H_4aobtc (left) and H_4sbtc (right). Hydrogen atoms were omitted for clarity. Color scheme: carbon, black; nitrogen, blue; oxygen, red.

corrections were applied using SADABS.[19] The structures were solved by direct methods and refined by full-matrix least-squares on F^2 with anisotropic displacement parameters for non-H atoms using SHELX-97.[20] The hydrogen atoms on the carbon were placed in calculated positions with isotropic displacement parameters set to $1.2U_{eq}$ of the attached atom. For PCN-10 and PCN-11, solvent molecules in the structure were highly disordered and impossible to refine using conventional discrete-atom models. To resolve these issues, the contribution of solvent–electron density was removed using the SQUEEZE routine in PLATON,[21] thereby producing a set of solvent-free diffraction intensities. The final formulas were calculated from the SQUEEZE results in combination with those of elemental analyses and TGA.

2.8. Low-Pressure Adsorption Measurements. Low-pressure volumetric gas adsorption measurements involved in this work were performed at 77 K, maintained by a liquid nitrogen bath, with pressures ranging from 0 to 760 Torr. Each sample was soaked in methanol for 24 h, and the extract was discarded. Fresh methanol was subsequently added, and the crystals were allowed to stay in methanol for an additional 24 h to remove solvates (DMA and H_2O). The sample was treated further with dichloromethane to remove methanol solvates. After decanting the dichloromethane extract, the sample was dried under a dynamic vacuum ($<10^{-3}$ Torr) at room temperature overnight. Before adsorption measurement, the sample was activated using the "outgas" function of the surface area analyzer for 2 h at 120 °C. In the hydrogen adsorption measurement, high-purity hydrogen (99.9995%) was used. The regulator and pipe were flushed with hydrogen before connecting to the analyzer. The internal lines of the instrument were flushed three times utilizing the "flushing lines" function of the program to ensure the purity of hydrogen.

2.9. High-Pressure Gas Adsorption Measurements and Analysis. High-pressure hydrogen and methane sorption isotherm measurements on PCN-10 and PCN-11 were performed using a home-built fully computer-controlled Sievert apparatus at NIST after an activation procedure similar to that in low-pressure volumetric gas adsorption measurements. The detailed specifications of the Sievert apparatus, data analysis, and discussion of excess adsorption can be found in a recently published work.[22] Briefly, the Sievert system is equipped with four different high-precision gauges (0.1%) and a closed-cycle cryostat, enabling adsorption measurements over a large pressure (0–50 bar) and temperature (30–300 K) range. Scientific/research-grade hydrogen and methane were used for the high-pressure measurements with purities of 99.9999% and 99.999%, respectively. Prior to measurements, solvent-exchanged samples were activated in two stages. First, the samples were outgassed under vacuum ($\sim 10^{-6}$ torr) overnight at room temperature, followed by heating at 120 °C for at least 4 h. Once the samples were activated, they were transferred to a He glovebox and never exposed to air. While still in the glovebox, approximately 200 mg of activated sample was loaded into the high-pressure cell, valved off with a He atmosphere, and then transported to the cryostat for measurement.

3. Results and Discussion

3.1. Synthesis and Structural Description of H_4sbtc and H_4abtc Ligands. H_4sbtc was synthesized in four steps from isophthalic acid through bromination, esterification, Heck reaction, and subsequent hydrolysis (Scheme 1), while

(19) *SAINT+*, version 6.22; Bruker Analytical X-Ray Systems, Inc.: Madison, WI, 2001.
(20) Sheldrick, G. M. *SHELX-97*; Bruker Analytical X-Ray Systems, Inc.: Madison, WI, 1997.

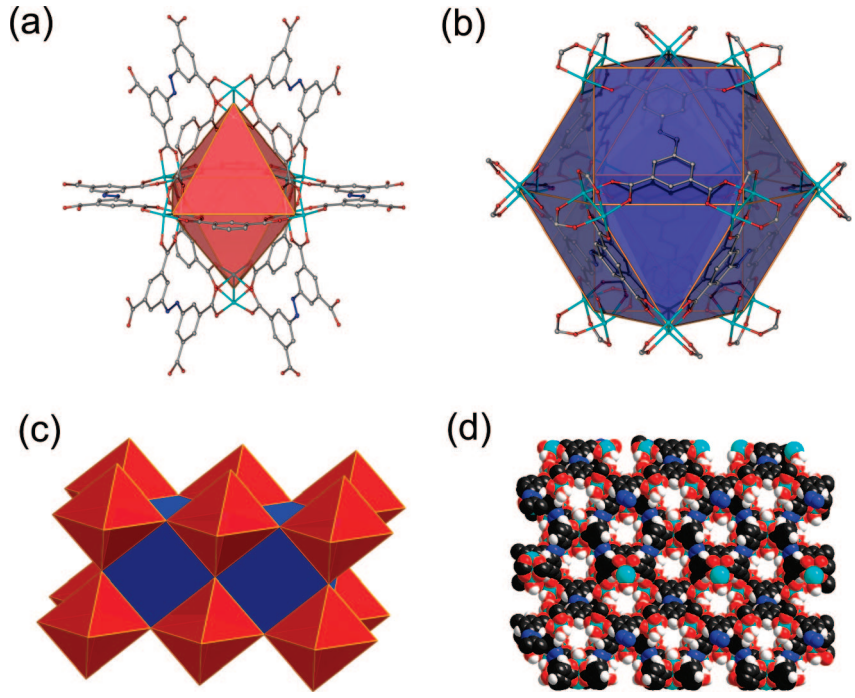

Figure 2. (a) Octahedral cage in PCN-10; (b) elongated cuboctahedral cage in PCN-10; the 3D framework of PCN-10 viewed as (c) polyhedron model; (d) space-filling model on the [0 15 13] plane. Color scheme: Cu, aqua; C, black; N, blue; O, red; and H, white.

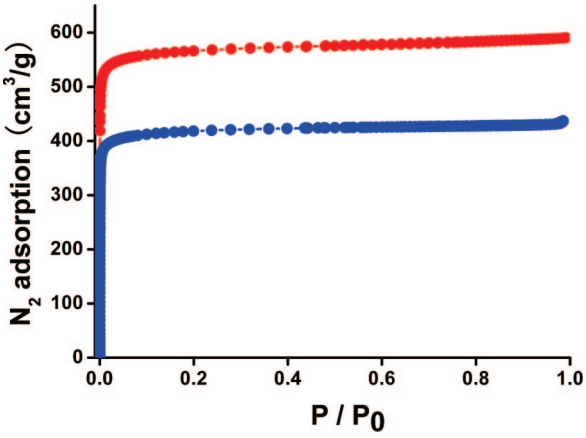

Figure 3. Dinitrogen adsorption isotherms for PCN-10 (blue) and PCN-11 (red).

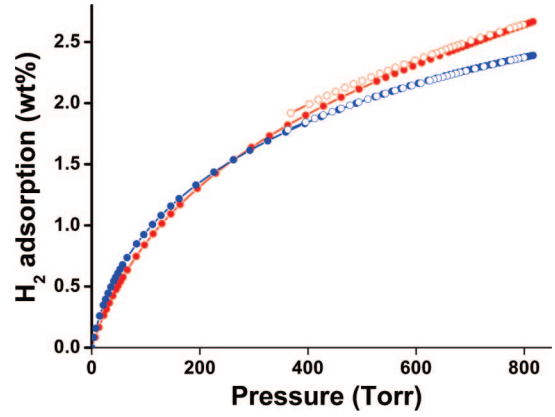

Figure 4. H_2 adsorption isotherms below 1.2 bar for PCN-10 (blue) and PCN-11 (red) at 77 K. Filled and open circles represent adsorption and desorption data, respectively.

the synthetic route for H_4aobtc is shown in Scheme 2. The ligand abtc was generated through reduction of the compound azoxybenzene-3,3′,5,5′-tetracarboxylate (aobtc) in the solvothermal reaction leading to PCN-10.

In the crystal structure of H_4aobtc, the N═N bond resides on an inversion center with the azoxy group disordered over two equally occupied orientations. Both the structures of H_4aobtc and H_4sbtc (Table 1) reveal planar structures with an average dihedral angle between the two benzene rings and the azoxy plane or ethene plane of 8.6° or 8.1°, respectively (Figure 1, Table 1). The distances between the isophthalic acid groups (between the 1 and 1′ positions) are 3.675 Å in aobtc and 3.764 Å in sbtc.

(21) Spek, A. L. *J. Appl. Crystallogr.* **2003**, *36*, 7.
(22) Zhou, W.; Wu, H.; Hartman, M. R.; Yildirim, T. *J. Phys. Chem. C* **2007**, *111*, 16131.

3.2. Synthesis and Structural Description of the PCNs. The reactions of $Cu(NO_3)_2$ with H_4aobtc or H_4sbtc in DMA gave two MOFs, or PCNs, $Cu_2(abtc)(H_2O)_2 \cdot 3DMA$ (PCN-10), and $Cu_2(sbtc)(H_2O)_2 \cdot 3DMA$ (PCN-11), respectively, which were characterized by X-ray crystallography, elemental analysis, and thermogravimetric analysis (TGA).

X-ray single-crystal structural analysis reveals that both PCN-10 and PCN-11 crystallize in the rhombohedral space group *R*-3 (Table 1). This is different from those of previously reported $[Cu_2L(H_2O)_2]$ MOFs,[15] which crystallize in *R*-3*m* space group, due to the lack of mirror plane perpendicular to the double bond in abtc and sbtc ligands. Because PCN-10 and PCN-11 are isostructural, the structural discussion will focus on PCN-10. In PCN-10, two copper atoms are linked by four bridging carboxylates to form a paddlewheel secondary building unit (SBU) and become coordinatively unsaturated upon removal of the axial water

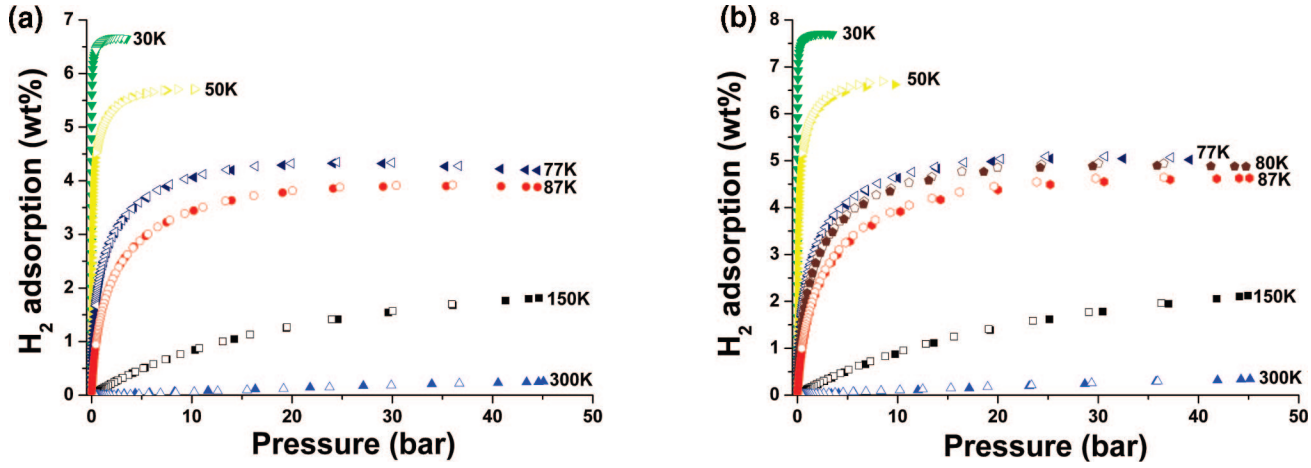

Figure 5. High-pressure hydrogen adsorption isotherms of PCN-10 and PCN-11 at multiple temperatures. (a) Excess adsorption isotherms of PCN-10; (b) Excess adsorption isotherms of PCN-11. Filled and open symbols represent adsorption and desorption data, respectively.

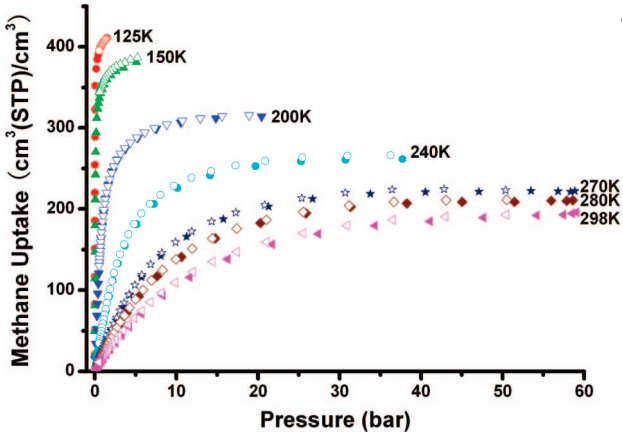

Figure 6. High-pressure methane excess uptake isotherms of PCN-11 at multiple temperatures. Filled and open symbols represent adsorption and desorption data, respectively.

ligands. Every 12 ligands connect 6 paddlewheel SBUs to form an octahedral cage with 8 triangular openings of 8.13 × 9.26 Å (Figure 2a) and about 900 Å^3 of space, providing an accessible interior surface for gas storage. Every eight octahedral cages connect to each other through vertex sharing to form an elongated cuboctahedral cage. The cuboctahedral cage consists of 6 ligands and 12 paddlewheel SBUs, with the 6 square faces occupied by the 6 ligands and the 8 triangular faces shared with 8 neighboring octahedral cages (Figure 2b, c). Each cuboctahedral cage connects 6 other cuboctahedral cages and 6 octahedral cages, leading to an extended NbO-type three-dimensional network with two types of oval-shaped channels. One type has an open window size of 8.13 × 9.26 Å on the [0, 15, 13] plane, and the other is 8.13 × 8.13 Å viewed from the *c* axis (Figure 2d, also see Supporting Information).

Since PCN-10 and PCN-11 are noninterpenetrated, high porosity can be expected. The solvent-accessible volumes, calculated using PLATON, are as high as 71.2% (PCN-10) and 71.9% (PCN-11) after being activated. The calculated density of structures after removal of solvent is 0.767 and 0.749 g/cm^3. TGA of polycrystalline samples of PCN-10 and PCN-11 revealed similar thermal behavior (see Supporting Information). Both samples showed that one discrete weight loss (about 36%) occurred at 25–250 °C, corresponding to removal of three DMA molecules per formula unit (37% calculated), the subsequent loss of coordinated aqua ligands (about 4.3%) of the copper paddlewheel SBU occurring from 250 to 310 °C. The framework is stable up to 310 °C, beyond which decomposition of the structures takes place. Both of the activated samples readily maintain porosity and structural integrity in a dry environment. However, once exposed to moisture, the sample disintegrates.

3.3. Low-Pressure Gas Sorption. The enduring porosity of PCN-10 and PCN-11 is confirmed by gas adsorption studies. To obtain the isotherms, blue-green block crystals of each MOF were soaked in methanol for 2 days to remove the DMA guest solvates. Afterward, the sample was soaked in dichloromethane for 3 days to remove methanol solvates. After decanting the extract, the sample was kept under a dynamic vacuum at room temperature overnight for activation, during which the crystal color shifted gradually to light blue. The aqua ligands on SBUs should remain in the framework at this stage. To remove the aqua ligands, samples were heated at 120 °C under a dynamic vacuum with the color of the sample shifting gradually to blue purple. Upon heating, PCN-11 retains its structure but PCN-10 partially decomposes upon activation (see Supporting Information). The N_2 adsorption isotherms of the activated samples exhibit type-I sorption behavior (Figure 3) with a Langmuir surface area of 1779 or 2442 m^2/g, corresponding to a BET surface area of 1407 or 1931 m^2/g and a total pore volume of 0.67 or 0.91 mL/g for PCN-10 or PCN-11, respectively. Because PCN-10 and PCN-11 are isostructural, one would expect that the activated samples of the two should have equal or similar surface areas. The significant reduction of surface area in PCN-10 is presumably due to the fact that an N═N double bond is thermally less stable than a C═C double bond.

The hydrogen sorption properties of PCN-10 and PCN-11 are shown in Figure 4. Neither sample shows evidence for saturation at 1 atm. In addition, the absence of adsorption–desorption hysteresis indicates that dihydrogen is reversibly adsorbed by PCN-10 and PCN-11. At 760 Torr and 77 K, PCN-10 adsorbs 2.34 wt % hydrogen (18.0 g/L), while PCN-11 adsorbs 2.55 wt % hydrogen (19.1 g/L). These

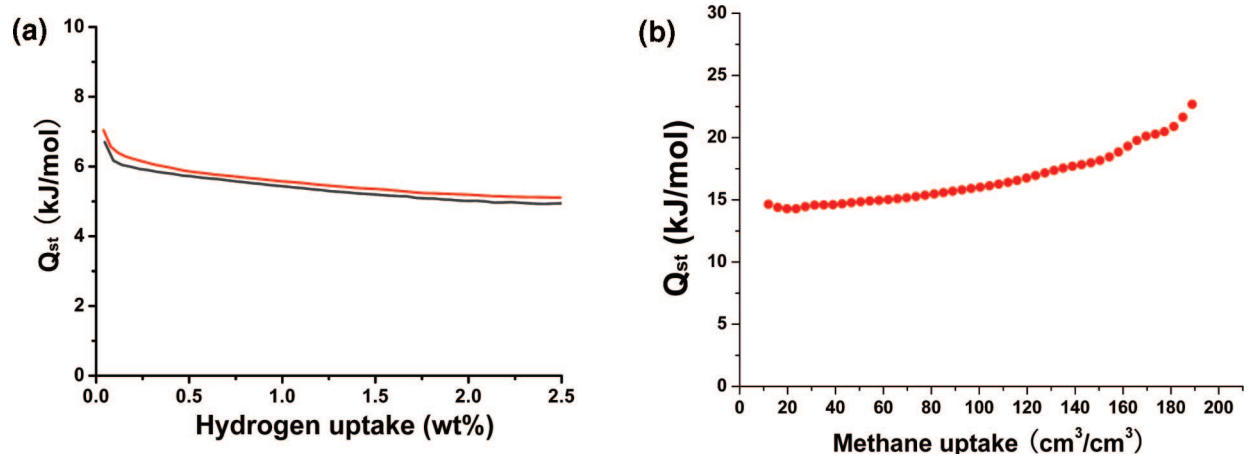

Figure 7. (a) Isosteric heats of hydrogen adsorption of PCN-10 (blue) and PCN-11 (red). (b) Isosteric heat of adsorption of methane of PCN-11.

hydrogen uptakes are among the highest reported for MOF materials.[14,15] The difference between the hydrogen uptakes of PCN-10 and PCN-11 is consistent with their corresponding surface areas, albeit at low coverage (less than 1.5 wt %), the small difference in uptake can be ascribed to the variation in the strength of interaction between the two different linkers and dihydrogen molecules, implying that the N═N double bond has higher H_2 affinity than that of the C═C double bond,[15j] consistent with a theoretical calculation.[7i]

3.4. High Pressure Hydrogen Sorption. Volumetric capacity is a significant parameter when comparing different storage materials. As shown in Figure 5, the maximum hydrogen adsorption of PCN-10 and PCN-11 is 52.5 (6.84 wt %) and 59.1 g/L (7.89 wt %) at 30 K, 3.5 bar, respectively. When temperature increases, the excess volumetric (gravimetric) adsorption in PCN-10 is 32.2 g/L (4.20 wt %) at 45 bar and 77 K and the total uptake is 39.2 g/L (5.23 wt %). Consistent with the trend shown in the low-pressure adsorption studies, the excess volumetric (gravimetric) adsorption of PCN-11 at 45 bar and 77 K is 37.8 g/L (5.04 wt %) and the total uptake reaches 44.7 g/L (5.97 wt %). The excess uptake is not far away from the highest observed in MOFs such as those in MOF-5 (42.1 g/L),[15i] $[M(CH_3OH)_6]_3[(M_4Cl)_3(BTT)_8]_2$ (43 g/L for Mn[15d] and 41 g/L for Cu[15e]), $[Cu_2L(H_2O)_2]$ MOFs (43.6 g/L for tpta and 41.1 g/L for qpta),[15b] and MOF-505 (38.9 g/L).[15a] The relatively high volumetric storage density of PCN-11, compared to its moderate gravimetric uptake, can be attributed to its higher density (0.749 g/cm^3), compared to superlight MOFs such as MOF-5 (0.593 g/cm^3)[12d] and MOF-177 (0.477 g/cm^3).[8a] However, at 300 K, the excess hydrogen uptakes of both PCN-10 and PCN-11 can only reach 0.25% and 0.34% at 45 bar, respectively, although the uptake may still increase if the pressure increases. The task of increasing the hydrogen affinity of MOFs at room temperature remains a challenge.

3.4.1. High Pressure Methane Sorption. To evaluate the methane-sorption properties of PCN-11, methane isotherms were measured in the pressure range of 0–60 bar at a variety of temperatures. The methane uptakes were directly converted into cm^3(STP)/cm^3 using the density of PCN-11 (0.749 g/cm^3) calculated from the crystal structure after axial ligand removal. As shown in Figure 6, all the adsorption and desorption isotherms follow the same trend, indicating typical type-I adsorption. At 125 K, methane uptake of PCN-11 is as high as 381 cm^3(STP)/cm^3. For application at 298 K and 35 bar, the excess uptake of methane for PCN-11 is 171 cm^3(STP)/cm^3, which represents 77% of the storage capacity of compressed methane cylinders (205 bar). The excess methane-adsorption capacity of PCN-11 approaches the DOE target of 180 cm^3(STP)/cm^3,[2] among the highest methane uptakes of all the reported porous materials.[6,12,13]

3.4.2. Analysis of Heat of Hydrogen and Methane Adsorption. To study the hydrogen affinity of PCN-10 and PCN-11, hydrogen adsorption isotherms were collected at 77 and 87 K. The isosteric heat of hydrogen adsorption was calculated using a modified version of the Clausius−Clapeyron equation.[23] As shown in Figure 7a, the enthalpies of hydrogen adsorption of PCN-10 and PCN-11 decrease from low coverage to high coverage in the range of 4–7 kJ/mol, similar to those of other reported MOFs.

The isosteric heats of methane adsorption (Q_{st}) were also calculated using the Clausius−Clapeyron equation[23] and isotherms taken at 270, 280, and 298 K. As shown in Figure 7b, the Q_{st} at low coverage is 14.6 kJ/mol, and the Q_{st} increases gradually as methane loading increases. This implies that the methane−methane interaction, in addition to the methane−framework interaction, becomes dominant at high methane loading, consistent with those of other reported MOF systems.[6c,22]

We note that the CH_4 heat of adsorption is much larger than that of H_2. This is expected because CH_4 is a larger molecule, and therefore, its interaction with the MOF host lattice is larger compared to interaction of hydrogen molecule. In fact, assuming that the same atom−atom van der Waals potential works for both CH_4 and H_2, we expect that the Q_{st} for CH_4 to be at about 5/2 (i.e., five atoms for CH_4 versus two atoms for H_2). Hence, the Q_{st} for CH_4 should be around 2.5 times larger than that for H_2. This approximate estimation gives a $Q_{st} \approx 15$ kJ/mol for CH_4 which is, in fact, what we measured as shown in Figure 7.

(23) Roquerol, F.; Rouquerol, J.; Sing, K. *Adsorption by Powders and Solids: Principles, Methodology, and Applications*; Academic Press: London, 1999.

4. Conclusions

Utilization of double-bond-coupled di-isophthalate ligands, H_4aobtc and H_4sbtc, in reactions with $Cu(NO_3)_2$ yielded two isostructural microporous MOFs, PCN-10 and PCN-11, respectively. Upon guest removal, both MOFs contain two types of pores, open metal sites, and retain enduring porosity. In particular, both contain nanoscopic cages that are particularly suitable for gas storage. At 760 Torr, 77 K, the excess hydrogen uptake of PCN-10 is 2.34 wt % (18.0 g/L) and that of PCN-11 is as high as 2.55 wt % (19.1 g/L). Gas-adsorption experiments suggest that MOFs containing C═C double bonds are more favorable than those with N═N double bond in retaining enduring porosity after thermal activation, although the N═N double bond has slightly higher H_2 affinity. When the pressure is increased, the excess adsorption at 77 K saturates around 20 atm and reaches values of 4.33% (33.2 g/L) and 5.05% (37.8 g/L) for PCN-10 and PCN-11, respectively. In addition, PCN-11 exhibits an excess methane uptake of 171 cm^3(STP)/cm^3 at 298 K and 35 bar, approaching the DOE target of 180 v(STP)/v for methane storage at ambient temperatures. Thus, PCN-11 represents one of the few materials that are applicable to both hydrogen and methane storage applications.

Acknowledgment. This work was supported by the U.S. Department of Energy (DE-FC36-07GO17033) and the U.S. National Science Foundation (CHE-0449634). H.-C.Z. acknowledges the Research Corporation for a Cottrell Scholar Award and Air Products for a Faculty Excellence Award. J.M.S. and T.Y. acknowledge support from the DOE (BES DE-FG02-98ER45701), and A.d.M. acknowledges support from the state of Nieder-sachsen.

Supporting Information Available: Crystallographic information file (CIF), TGA curves, and XRD patterns of PCN-10 and PCN-11; additional crystal structure figures of PCN-11 and ^{13}C NMR and ^{1}H NMR spectra of tetramethyl *trans*-stilbene-3,3′,5,5′-tetracarboxylate (PDF). This material is available free of charge via the Internet at http://pubs.acs.org.

CM800403D